A&A 497, 177–181 (2009)
DOI: 10.1051/0004-6361/200911655
© ESO 2009

Astronomy & Astrophysics

CO in OH/IR stars close to the Galactic centre *(Research Note)*

A. Winnberg[1], S. Deguchi[2], M. J. Reid[3], J. Nakashima[4,5], H. Olofsson[1,6], and H. J. Habing[7]

[1] Onsala Space Observatory, Observatorievägen, 439 92 Onsala, Sweden
e-mail: anders.winnberg@chalmers.se
[2] Nobeyama Radio Observatory, Minamisaku, Nagano 384–1305, Japan
[3] Harvard-Smithsonian Center for Astrophysics, 60 Garden Street, Cambridge MA 02138, USA
[4] Academia Sinica Institute of Astronomy and Astrophysics, PO Box 23–141, Taipei 106, Taiwan
[5] Department of Physics, University of Hong Kong, Pokfulam Road, Hong Kong
[6] Stockholm Observatory, AlbaNova University Centre, 106 91 Stockholm, Sweden
[7] Sterrewacht Leiden, PO Box 9513, 2300 RA Leiden, The Netherlands

Received 13 January 2009 / Accepted 9 February 2009

ABSTRACT

Aims. A pilot project has been carried out to measure circumstellar CO emission from three OH/IR stars close to the Galactic centre. The intention was to find out whether it would be possible to conduct a large-scale survey for mass-loss rates using, for example, the Atacama large millimeter array (ALMA). Such a survey would increase our understanding of the evolution of the Galactic bulge.
Methods. Two millimetre-wave instruments were used: the Nobeyama Millimeter Array at 115 GHz and the Submillimeter Array at 230 GHz. An interferometer is necessary as a "spatial filter" in this region of space because of the confusion with *inter*stellar CO emission.
Results. Towards two of the stars, CO emission was detected with positions and radial velocities coinciding within the statistical errors with the corresponding data of the associated OH sources. However, for one of the stars the line profile is not what one expects for an unresolved expanding circumstellar envelope. We believe that this CO envelope is partially resolved and that this star therefore is a foreground star not belonging to the bulge.
Conclusions. The results of the observations have shown that it is possible to detect line profiles of circumstellar CO from late-type stars both within and in the direction of the Galactic bulge. ALMA will be able to detect CO emission in short integrations with sensitivity sufficient to estimate mass-loss rates from a large number of such stars.

Key words. stars: AGB and post-AGB – stars: circumstellar matter – stars: mass-loss – Galaxy: bulge – radio lines: ISM – techniques: interferometric

1. Introduction

Rapid stellar mass loss occurs at the so-called red giant and, in particular, the asymptotic giant branches (RGB and AGB). Due to high stellar density and rapid star formation, the Galactic bulge contains large numbers of RGB and AGB stars. It is important to measure the mass-loss rates of these stars for a picture of the recirculation of matter and metal enrichment in this region of the Milky Way. In addition, stars in the central bulge are at distances that differ from one another by merely a few percent leading to an accurate estimate of the mass-loss-rate *distribution*.

The most accurate method of estimating the stellar mass-loss rates is based on the CO rotational spectral lines (cf. Ramstedt et al. 2008). The first attempt to detect such circumstellar lines in the vicinity of the Galactic centre (GC) was made by Mauersberger et al. (1988) using the IRAM 30-m telescope. They detected the $J = 1 \rightarrow 0$ and $2 \rightarrow 1$ CO lines from the proto-planetary nebula (PPN) OH0.9+1.3 which has a high radial velocity (–110 km s^{-1}) making it likely to be physically close to the GC. They also proposed to look for CO emission from OH/IR stars, since such stars are believed to be the progenitors of PPNe. Winnberg et al. (1991) used the same radio telescope to observe several OH/IR stars close to the GC but detected CO emission from only one star: OH0.3–0.2 (Baud et al. 1975). This star has a very high radial velocity (–341 km s^{-1}) and therefore the circumstellar emission is not affected by the interstellar background emission that covers typically the velocity range –200 to +200 km s^{-1}. None of the other candidate stars were detected because of confusion with interstellar emission.

The present project employs a different observing technique in an attempt to detect the *circum*stellar CO emission in the midst of *inter*stellar CO emission. A radio interferometer with suitable baselines can be used as a "spatial filter" by resolving most of the interstellar background but leaving the circumstellar emission as unresolved point sources.

To determine optimal baseline lengths and the most favourable CO lines, we started a pilot experiment. We chose three OH/IR stars close to the position of the GC with strong IR fluxes and with low-to-moderate radial velocities. In 2003–2004 we used the Nobeyama millimeter array (NMA) at 115 GHz (CO, $J = 1 \rightarrow 0$) and in 2005 we used the SubMillimeter Array (SMA; Mauna Kea, Hawaii) at 230 GHz ($J = 2 \rightarrow 1$).

This research note presents the main results of these two data sets and outlines the prospects for future systematic surveys of

Table 1. Selected OH/IR stars.

Name	RA (J2000)	Dec (J2000)	V_{rad} (km s^{-1})	V_{exp} (km s^{-1})	$F_{[15]}$ (Jy)	Ref.
OH0.3–0.2	$17^h47^m\,06.95^s$	$-28°\,44'\,42.2''$	–341.0	14.5		1
OH359.117–0.169	$17^h47^m\,21.79^s$	$-29°\,47'\,42.2''$	–88.5	21.2	6.9	2
OH359.762+0.120	$17^h44^m\,34.95^s$	$-29°\,04'\,35.2''$	–5.7	15.3	13.8	3
OH359.971–0.119	$17^h46^m\,00.94^s$	$-29°\,01'\,23.6''$	–8.5	19.3	9.5	3

References: 1. Fix & Mutel (1984); 2. Sevenster et al. (1997); 3. Lindqvist et al. (1992).

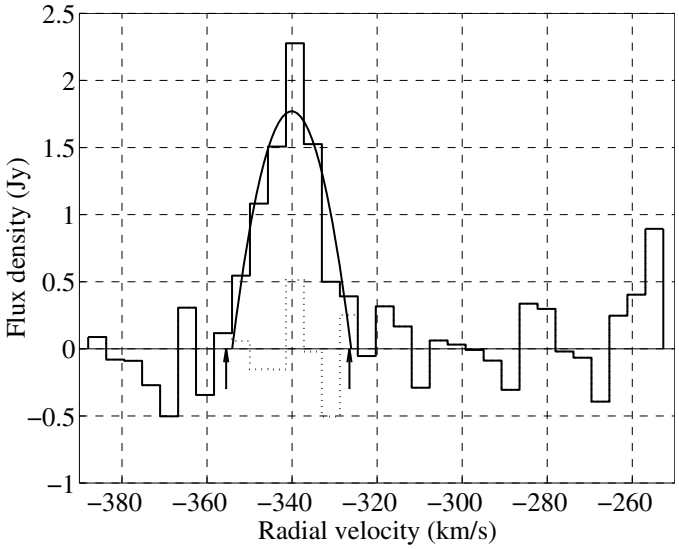

Fig. 1. Circumstellar CO(2 → 1) line profile of OH0.3–0.2. The thick "staircase" line is the observed spectrum; the thick curved line is a fitted parabola; the dotted line depicts the residuals (i.e., observed spectrum minus parabola). The arrows indicate the velocities of OH masers.

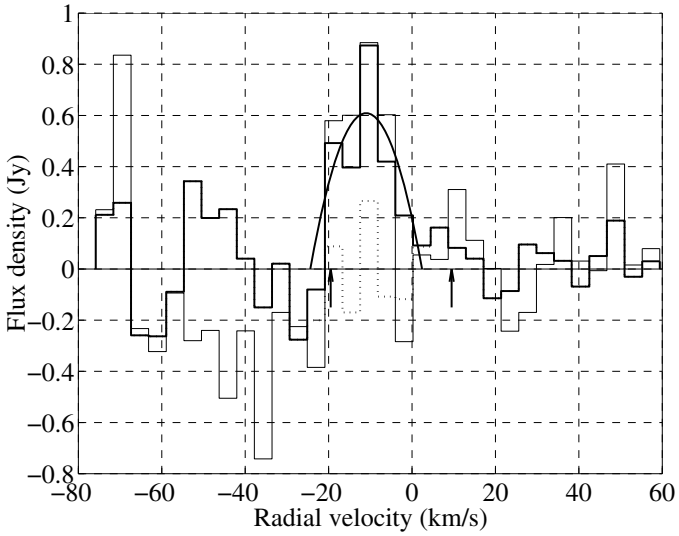

Fig. 2. Circumstellar CO(2 → 1) line profiles of OH359.762+0.120. The thick "staircase" line is the observed spectrum with baseline lengths shorter than 25 kλ excluded. The parabola, the residuals and the OH maser velocities are represented as in Fig. 1. In addition, a thin "staircase" line indicates an observed spectrum with all projected baseline lengths included.

late-type stars in the Galactic bulge using the Atacama large millimeter array (ALMA). A conference report of this project appears in Winnberg et al. (2006).

2. Observations

The first observations in this project were done with the 6-element array (NMA) at Nobeyama Radio Observatory, Japan, in November 2003 and in January 2004 at 115 GHz. Three OH/IR stars were selected for observations on the basis of strong IR fluxes: OH359.117–0.169, OH359.762+0.120 and OH359.971–0.119 (Ortiz et al. 2002). The relevant data for these stars are listed in Table 1, where $F_{[15]}$ denotes the flux density at a wavelength of 15 μm as measured by the Infrared Space Observatory (ISO). A clear signal was obtained from OH359.971–0.119 (Fig. 3, dotted line). The position of the CO line agreed with the position of the 1612-MHz OH line. However, the line width was too narrow for an unresolved circumstellar CO source and the radial velocity of the line was close to that of the red-shifted OH line component rather than to the average velocity of the two OH components.

Data were taken using two digital correlation spectrometers simultaneously. One of them consisted of 128 channels with a width of 8.0 MHz. The other one had 1024 channels of width 31.25 kHz.

In June 2005 the same three stars plus the previously detected star OH0.3–0.2 were observed using the 8-element array (SMA) on Mauna Kea, Hawaii, at 230 GHz. The spectrometer was configured to give a resolution of 3.25 MHz. The test star OH0.3–0.2 was detected and showed properties in accordance with the single-dish data (Fig. 1). In addition the stars OH359.762+0.120 and OH359.971–0.119 were detected (Figs. 2 and 3).

Typical synthesized beam FWHM values of images produced with all baselines were $4'' \times 7''$ for the NMA and $3'' \times 4''$ for the SMA.

3. Data reduction

3.1. The NMA

The data were calibrated using the Nobeyama internal programme package and subsequently the astronomical image processing system (AIPS) was used in a standard way to obtain images and spectra.

We found strong ripples in the images that could be eliminated by removing data from projected baselines shorter than 10 kλ (26 m). Due to atmospheric phase instability, we decided to remove all projected baselines longer than 40 kλ (104 m) and to introduce a gaussian baseline-length taper such that baselines of length 40 kλ got a weight of 30%.

Table 2. Results.

Name	Trans. (J)	RA (J2000)	Dec (J2000)	V_m (km s^{-1})	V_e (km s^{-1})	S_m (Jy)	$\dot{M}$ ($M_\odot$ yr^{-1})
OH0.3–0.2	2 → 1	$17^h47^m\,06.978^s(0.009)$	−28° 44′ 42.8″(0.2)	–340.1(0.6)	14.0(0.8)	1.8(0.1)	5×10^{-4}
OH359.117–0.169	1 → 0					≲0.2	
	2 → 1					≲0.54	
OH359.762+0.120	1 → 0					≲0.15	
	2 → 1	$17^h44^m\,34.979^s(0.012)$	−29° 04′ 36.6″(0.2)	–11(1)	13(1)	0.6(0.1)	4×10^{-4}
OH359.971–0.119	1 → 0	$17^h46^m\,00.75^s$ (0.04)	−29° 01′ 21.5″(0.7)			∼0.4	
	2 → 1	$17^h46^m\,00.909^s(0.008)$	−29° 01′ 23.2″(0.2)			∼5	

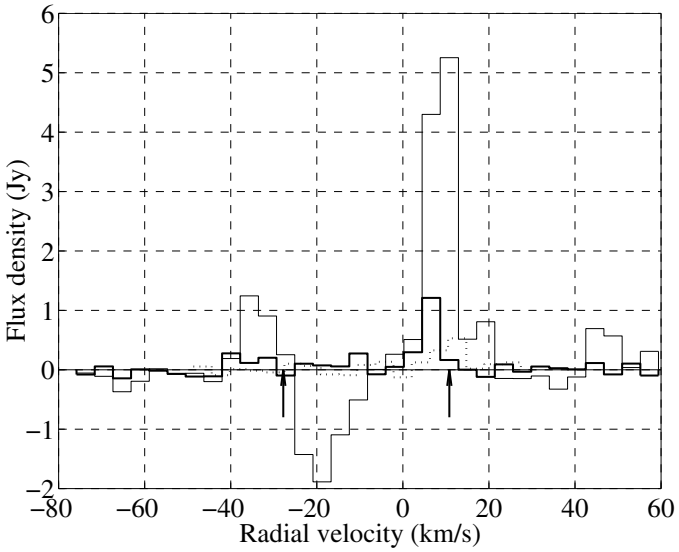

Fig. 3. Circumstellar CO(2 → 1) line profiles of OH359.971–0.119. The definitions of the lines are given in the caption of Fig. 2, except in this figure the dotted "staircase" line is the CO(1 → 0) spectrum as observed with the NMA.

Maps were made with 256 × 256 pixels of size 0.5″ with uniform weighting. They were "cleaned" using the standard Högbom/Clark algorithm with a gain of 0.1 and a minimum flux density per clean component being the product of the beam dynamic range (1/|strongest sidelobe|) and the expected rms noise fluctuations. This ensured that no "overcleaning" took place in the rather noisy maps.

Data cubes were made consisting of images from the 20 central channels of the low-resolution spectrometer covering 416 km s^{-1}. For the high-resolution spectrometer similar data cubes were made consisting of 256 channels where each channel resulted from averaging 4 original channels. Therefore these spectra covered 83.2 km s^{-1} with a resolution of 0.325 km s^{-1}.

3.2. The SMA

Data from this instrument were retrieved using software from the Radio Telescope Data Center (RTDC) of the Center for Astrophysics (CfA). Calibration was performed using the image processing package IDL-MIR at Academia Sinica Institute of Astronomy and Astrophysics (ASIAA). Further data reduction was made using both AIPS at Onsala Space Observatory (OSO) and MIRIAD (SMA version) at ASIAA.

The *uv* data were investigated for the presence of spatially extended emission by plotting the visibility amplitude as a function of projected baseline length. Based on such plots it was decided to exclude baselines shorter than 25 kλ (32.5 m) for OH359.762+0.120 and shorter than 30 kλ (39 m) for OH359.971–0.119 in order to avoid, as far as reasonable, contamination by residuals of interstellar emission. For OH359.117–0.169 no evidence of significant interstellar emission was found. No interstellar emission was found in the IF band of the test source OH0.3–0.2 as expected.

Map-cubes were made with 256 × 256 pixels of size 0.5″, however, this time with natural weighting. They were "cleaned" using the standard Högbom/Clark algorithm in a manner similar to the treatment of the NMA data. When a compact source was seen in one of the channels within the OH velocity span at a position close to the position of the OH source, we fitted a two-dimensional elliptical Gaussian and extracted a spectrum at the pixel closest to this position.

After exclusion of the shorter baseline lengths all the maps are free from interstellar CO emission except for occasional point sources. We interpret them as unresolved rests of interstellar emission. Since most of the emission is resolved there are "negative point sources" as well, i.e. unresolved "dips" in the interstellar background. The positions of the OH/IR stars are known to 1″ or better, and therefore there is never any doubt about the identification of a circumstellar CO source. In addition to the position evidence, there is the radial velocity evidence that strengthens the identification case quite considerably.

4. Results

Table 2 lists the measured parameters of the CO sources associated with the four stars observed. The 1-σ errors are given in parentheses after the values. For OH0.3–0.2 and OH359.762+0.120 (2 → 1) least-square fits of parabolas to the CO line profiles have been made, assuming that the data are from unresolved, optically thick emission:

$$S = S_m\left[1-\left(\frac{V-V_m}{V_e}\right)^2\right] \quad (1)$$

where S_m is the maximum flux density at the radial velocity V_m, and V_e is half the line width at zero intensity. These three parameters are given in the table together with the statistical errors from the fitting procedure. No CO emission associated with OH359.117–0.169 (1 → 0 and 2 → 1) and OH359.762+0.120 (1 → 0) was found and 3-σ upper limits are given for S_m. The CO line profiles for OH359.971–0.119 (1 → 0 and 2 → 1) are incompatible with a parabola, although the CO positions are

coincident with the OH position, and only approximate values of the maximum flux densities are given (Fig. 3).

OH359.117–0.169 was not detected at any of the two CO lines and we do not know the reason for it. One guess would be that this is due to heavy absorption by interstellar CO clouds in front of the star. Such a case could possibly occur for a star that is situated at a distance beyond the GC.

OH359.762+0.120 was detected with a rather poor S/N. Therefore there are quite large errors associated with the elements of the fitted parabola (Fig. 2 and Table 2). Within these errors, the mean radial velocity of the line and the line width are compatible with the systemic velocity of the star and its envelope expansion velocity as measured from the OH line profile. Notice that the exclusion of short baselines did not improve the detection of the line significantly. It merely improved the spectral baseline.

OH359.971–0.119 was detected with moderate to good S/N. However, the CO line is narrow and close to the "red-shifted" OH line component, i.e. the backside of the envelope (Fig. 3). A similar, but considerably weaker, line was observed with the NMA at 115 GHz (dotted line). Notice that the line profile obtained when all the *uv* data were included (thin solid line) shows a much stronger and broader "red-shifted" line and even a "blue-shifted" counterpart. The "negative signal" near -20 km s^{-1} is probably caused by a "dip" in the interstellar background, as discussed above, but in this case it is resolved.

Mass-loss rates have been calculated for OH0.3–0.2 and OH359.762+0.120 ($2 \rightarrow 1$) using a new formula based on the original equation by Knapp & Morris (1985) but containing constants determined by least-squares fits to physical models (Ramstedt et al. 2008), and the values have been entered in Table 2. For these calculations a distance of 8 kpc to the GC (Reid, 1993) and a CO/H_2 abundance ratio of 2×10^{-4} (Ramstedt et al. 2008) have been assumed for both stars. The values of V_e have been taken as the expansion velocities of the CSEs. Both mass-loss rates are normal for OH/IR stars (we caution that the validity of the Ramstedt et al. formula has only been tested in the mass-loss-rate range 10^{-7} to 10^{-5} $M_\odot$ yr^{-1}).

5. Discussion

5.1. OH359.762+0.120

There is little doubt, in spite of the poor S/N, that the detected CO source is a true circumstellar source associated with the OH/IR star. Because of the high bolometric magnitude of this star and its strong OH emission, some people doubt the association of this star with the Galactic bulge (see discussion by Blommaert et al. 1998). However, as pointed out by Blommaert et al. (1998), the OH radiation is heavily scattered by interstellar free electrons (Frail et al. 1994) making it very likely that it resides close to the GC. Our result of a weak CO source leading to a normal mass-loss rate for an assumed distance of 8 kpc supports this conclusion.

5.2. OH359.971–0.119

This star (as well as OH359.762+0.120) has detected 43-GHz SiO emission (Lindqvist et al. 1991). However, the $v = 2$, $J = 1 \rightarrow 0$ SiO line is much stronger than its $v = 1$ counterpart. This suggests a cool dust temperature and a high mass-loss rate (Nakashima & Deguchi 2007).

The CO source associated with this star, on the other hand, is an enigma. The line profile is similar to that expected from a well-resolved circumstellar envelope where unresolved emission is left at the front and back sides (see for example the central CO source in U Cam, Lindqvist et al. 1999). For such a picture to be true, the star needs to be at a small distance and would not belong to the Galactic bulge. For example, assuming that the diameter of the CO envelope is 2×10^{17} cm (which might be an overestimate for the $2 \rightarrow 1$ transition) and that the angular diameter is $10''$, the distance would be only about 1.4 kpc. The IR properties of this star also are such that it is arguable whether it belongs to the bulge (cf. Ortiz et al. 2002).

Another explanation of the line profile would be that it is heavily distorted through strong absorption of interstellar CO in front of the source. A third possibility – although improbable – is that the physical conditions in this CSE are such that they favour weak maser action along radial directions (Morris, 1980). Finally, there remains the (improbable) explanation that the source is an unresolved remnant of interstellar CO emission that happens to be at the same position and radial velocity as OH359.971–0.119.

Observations of higher-energy CO lines might be a possible way of revealing the true nature of this source. However, given the available data, we favour the first alternative, i.e. that we have found a relatively nearby OH/IR star whose CO envelope is resolved by both arrays used. The salient points that support this conclusion are:

- there are two CO line components whose positions and radial velocities correspond to those of the OH line components;
- the redshifted CO line component grows stronger and the blueshifted line component emerges when all baselines (including the short ones) are included in the imaging;
- there is a weak line component at 115 GHz whose radial velocity coincides with that of the redshifted 230-GHz component and whose position coincides with that of the OH/IR star;
- the 115-GHz line is much weaker than the 230-GHz counterpart which mostly is the case for circumstellar CO lines in OH/IR stars especially those with cool CSEs (Heske et al. 1990).

6. Conclusions

Our pilot project has shown that it is possible to detect circumstellar CO envelopes of OH/IR stars close to the GC: out of three stars selected, one was detected at both 115 and 230 GHz (OH359.971–0.119) and another one was detected at 230 GHz only (OH359.762+0.120). OH359.971–0.119 probably does not belong to the Galactic bulge, but this fact is irrelevant for the issue at stake – this star too would have been hard to detect using a single-dish telescope.

We would have liked to observe the same three stars at 345 GHz ($J = 3 \rightarrow 2$) and to try out somewhat longer baselines, but both these requests require excellent atmospheric conditions and therefore the competition for observing time is strong.

We have no doubt that ALMA will be able to detect a large number of OH/IR stars in the inner bulge (Olofsson 2008).

Acknowledgements. A.W. thanks the National Radio Observatory of Japan for a Visiting Professorship during the observations at Nobeyama. The NMA is operated by Nobeyama Radio Observatory, a branch of National Astronomical Observatory of Japan. The SMA is a joint project between the Smithsonian Astrophysical Observatory and the Academia Sinica Institute of Astronomy and Astrophysics and is funded by the Smithsonian Institution and the Academia Sinica.

References

Baud, B., Habing, H. J., O'Sullivan, J. D., Winnberg, A., & Matthews, H. E. 1975, Nature, 258, 406

Blommaert, J. A. D. L., van der Veen, W. E. C. J., van Langevelde, H. J., Habing, H. J., & Sjouwerman, L. O. 1998, A&A, 329, 991

Fix, J. D., & Mutel, R. L. 1984, Astron. J., 89, 406

Frail, D. A., Diamond, P. J., Cordes, J. M., & van Langevelde, H. J. 1994, ApJ, 427, L43

Heske, A., Forveille, T., Omont, A., van der Veen, W. E. C. J., & Habing, H. J. 1990, A&A, 239, 173

Knapp, G. R., & Morris, M. 1985, ApJ, 292, 640

Lindqvist, M., Ukita, N., Winnberg, A., & Johansson, L. E. B. 1991, A&A, 250, 431

Lindqvist, M., Winnberg, A., Habing, H. J., & Matthews, H. E. 1992, A&AS, 92, 43

Lindqvist, M., Olofsson, H., Lucas, R., et al. 1999, A&A, 351, L1

Mauersberger, R., Henkel, C., Wilson, T. L., & Olano, C. A. 1988, A&A, 206, L34

Morris, M. 1980, ApJ, 236, 823

Nakashima, J., & Deguchi, S. 2007, ApJ, 669, 446

Olofsson, H. 2008, Astrophys. & Space Sci., 313, 201

Ortiz, R., Blommaert, J. A. D. L., Copet, E., et al. 2002, A&A, 388, 279

Ramstedt, S., Schöier, F. L., Olofsson, H., & Lundgren, A. A. 2008, A&A, 487, 645

Reid, M. J. 1993, ARA&A, 31, 345

Sevenster, M. N., Chapman, J. M., Habing, H. J., Killeen, N. E. B., & Lindqvist, M. 1997, A&AS, 122, 79

Winnberg, A., Lindqvist, M., Olofsson, H., & Henkel, C. 1991, A&A, 245, 195

Winnberg, A., Deguchi S., Habing, H. J., et al. 2006, J. Phys. Conf. Ser., 54, 166